Chapter-2

A Low-Cost Solution Processed PTB7 Based MSM Visible Photodetector

The Part of the work is adopted from-

J. S. Rana, and S. Jit, "**A Low-cost Solution Processed PTB7 based MSM Visible Photodetector** ," ***IEEE Photon. Trans Devices***, vol. 71, no. 2, pp. 1208-1213, Feb. 2024, doi: 10.1109/TED.2023.3344547.

2.1 Introduction

Organic semiconducting materials-based electronic devices are most favourable for various applications including photodetection and gas sensing as discussed in Chapter 1. The visible photodetector, a type of photodetector, is an emerging device for visible light communication (VLC) for future generation 5G wireless network communication systems [106][107]. Thus, photodetectors operating in the visible range are an integral part of VLC-based wireless communication systems. Therefore, many researchers are focussing on fabricating low-cost visible range photodetectors (VPs) for VLC applications [108][109][110][111]. Researchers have explored both inorganic [112][113] and organic materials [36][70][114] materials for fabricating the visible range photodetectors. However, the organic thin film-based photodetectors have drawn considerable attention for VLC applications because the large-area organic thin films can be easily deposited on different substrates using different low-cost, low-temperature methods such as thermal evaporation, spin coating, inkjet printing and spray coating [115]. Among the aforementioned methods, the spin coating is perhaps the most widely explored solution-based fabrication technique for obtaining the large-area organic thin films for various electronic and optoelectronic applications.

As discussed in Chapter 1, PTB7-based photodetector can effectively detect visible light. Among various photodetector structures, MSM photodetectors have been widely studied for their ease of fabrication, and large bandwidth. Therefore, PTB7-based MSM photodetector is investigated in this chapter. The current section of Chapter 2 discusses the introduction of the chapter. Section 2.2 includes the experimental details used for the fabrication MSM photodetector device. In the subsequent section, results and discussion are presented. Finally, in the last section, the conclusion of this chapter is included.

2.2 Experimental Details

2.2.1. Substrate Cleaning and SiO_2 Growth

Sigma Aldrich supplied high-purity chemicals (99.99%) used in the device fabrication and the polymer PTB7 has been purchased from Ossila Ltd. (UK). The boron-doped p^+ Si substrates (resistivity, 2-5 Ω-cm) were cleaned using standard Radio Corporation of America (RCA)-1 followed by RCA-2 methods. The Si substrates were first cleaned with soap solution followed by cleaning with Trichloroethylene (TCE) and then they were sonicated for 10 minutes. After that, the samples were washed in running DI water (from Millipore, Milli-Q, USA). The substrates were further cleaned with isopropyl alcohol followed by acetone in an ultrasonic bath for 10 minutes each and at last again cleaned with DI water. Impurities, if any, were removed by dipping the samples into Pirhana solution (H_2O_2:H_2SO_4::60:40) for 10 min followed by dipping them into HF:DI (1:9) solution for 10 min to remove the native oxides, if any, from the surface of the Si substrates. After cleaning the samples with DI water, dried in the oven for 15 min. Before processing for the growth of SiO_2 on the cleaned Si substrates, they were placed in oxygen plasma cleaner for 10 min. The samples were then placed in the quartz chamber of the oxidation furnace at temperature 1100 °C for ~4 hours for SiO_2 layer growth (~300 nm thickness) on the Si substrates for photodetector fabrication.

2.2.2. Device Fabrication

The PTB7 polymer was mixed in Dichlorobenze (5 mg/ml) and the resultant solution was vigorous stirred at 50 °C for 10 hours to obtain a uniform solution of PTB7 for thin film preparation. The polymer solution was spin-coated on the SiO_2 layer Si substrate at 2000 rpm for 45 seconds, achieved the polymer thin film of ~60 nm thickness (measured by Filmetrics F-20, thin film analyzer). The PTB7-coated samples were then annealed for 45 minutes at 90 °C in ambient conditions to evaporate solvent from the film. Al metal was

deposited on polymer film at ~10^{-6} torr vacuum level and ~0.3 nm/s deposition rate to get metal contact, thickness of ~110 nm thickness with effective area ~0.0003 cm^2 (shown in Fig. 2) using shadow masks in thermal coating unit (HH-VAC, Model BL300). The channel length of the device was 30 μm. The post-annealing was performed after electrode deposition for 10 min. at 90 °C in ambient conditions.

Various steps of the fabrication process are demonstrated in **Figure 2.1**, while the fabricated device and its schematic structure are represented in **Figure 2.2(a)** and **(b)**, respectively.

2.3 Results and Discussions

2.3.1. Surface Morphology of the PTB7 Film

The surface morphology of the polymer thin film was analyzed by AFM (NTEGRA Prima) image shown in **Figure 2.3**. The AFM image shows a uniform polymer film with an average surface roughness of ~0.440 nm ± 0.146 nm.

2.3.2. Optical Characterization of the PTB7 Thin Film

Optical absorption characteristics of the PTB7 film were studied by UV-visible spectroscopy (JASCO, V730 from Japan) shown in **Figure 2.4(a)**. The PTB7 thin film is found to mostly absorb visible light, with the dominant absorption between 640 and 670 nm. The energy bandgap (~1.64 eV) of the solution-processed PTB7 film under study is estimated from the tauc plot shown in **Figure 2.4(b)**.

2.3.3. Optical Characterization of Fabricated Device

The current-voltage (I-V) characteristics of the proposed PTB7-based MSM photodetector have been measured by using a semiconductor parameter analyzer (Model B1500A USA, Keysight) and monochromator (Camlin ATLAS 300).

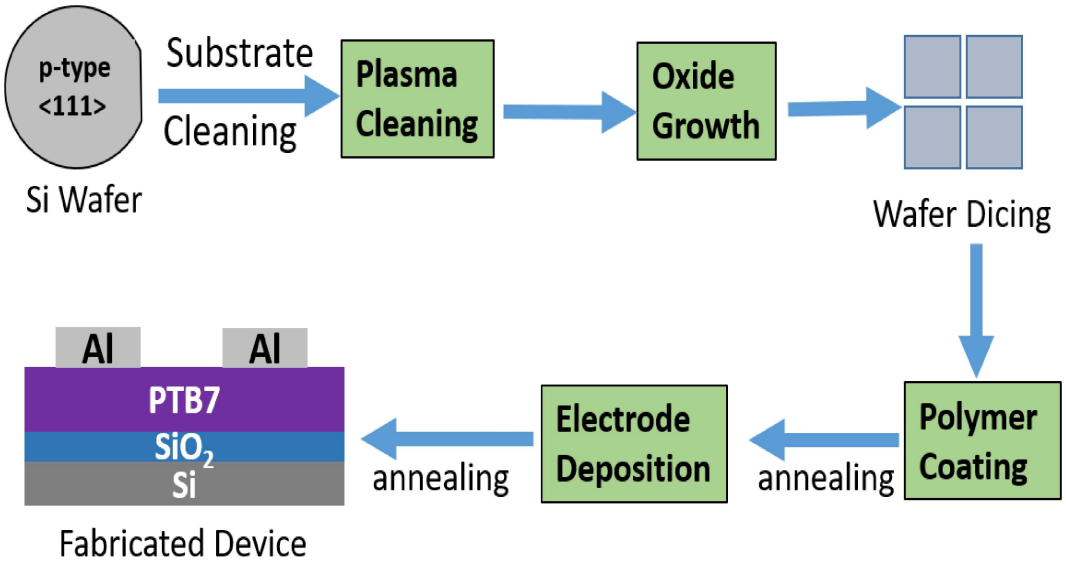

Figure 2.1 Fabrication steps used for device fabrication.

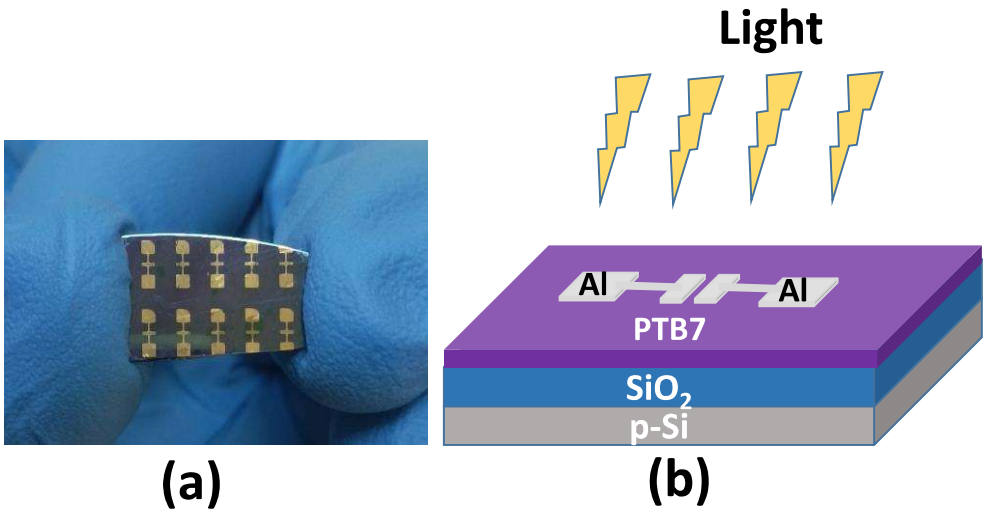

Figure 2.2 Fabricated device image and device schematics are shown (a) and (b).

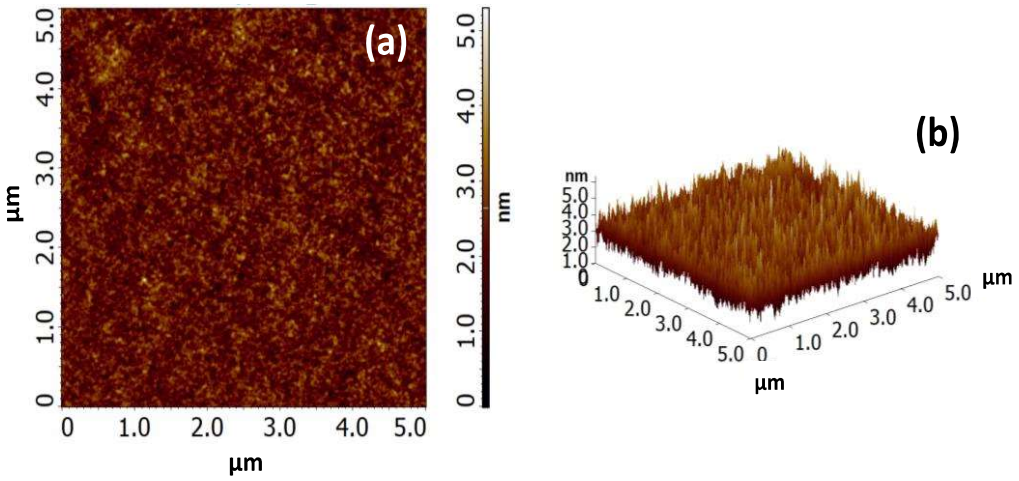

Figure 2.3 AFM image of the polymer thin film (a) 2D and (b) 3D for surface morphology analysis.

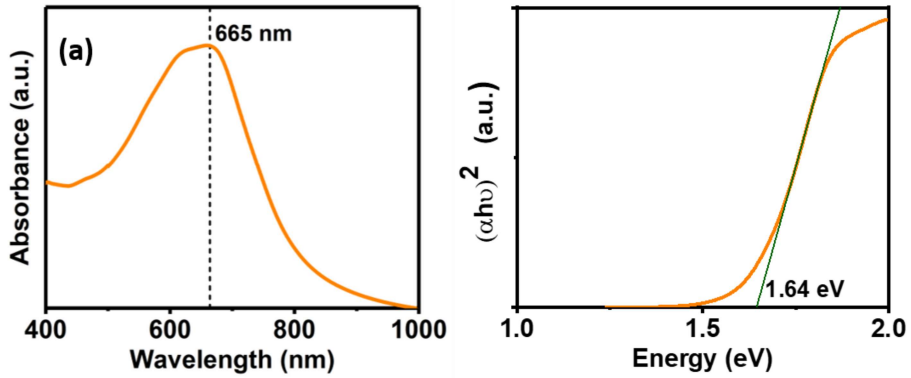

Figure 2.4 (a) UV-Vis spectrum of the polymer film and (b) band gap calculation.

The room-temperature (~25 °C) I-V characteristics under dark and illumination (Xenon Source) are shown in **Figure 2.5(a)** for -3 V to 3 V bias voltage. The symmetric nature of the I-V characteristics shown in **Figure 2.5** confirms the MSM photodetector structure (similar to two schottky diodes connected in back-to-back configuration) of our proposed device [116][117]. The maximum currents under light (I_{light}) and dark (I_{dark}) conditions were obtained as ~1.09 µA and ~140 nA at -3 V, respectively.

The measured responsivity (R) versus wavelength characteristic of the proposed photodetector is shown in **Figure 2.5(b)**. It is computed by using the following expression [118][119]:

$$R = \frac{Photocurrent}{Incident\ Optical\ Power} = \frac{I_{ph}}{P_{opt}} \tag{2.1}$$

where I_{ph}, and P_{opt} are the photocurrent and incident optical power, respectively. The photocurrent (I_{ph}) is obtained as:

$$I_{ph} = I_{light} - I_{dark} \tag{2.2}$$

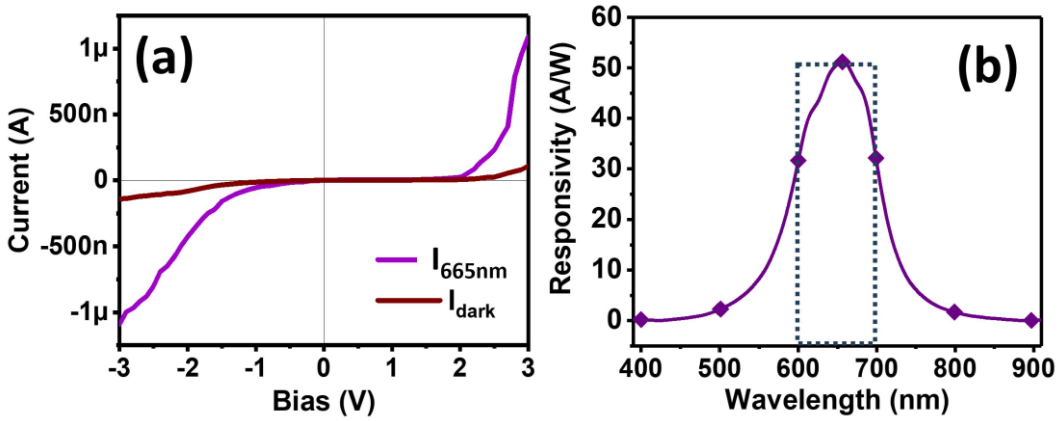

Figure 2.5 (a) I-V measurements of the fabricated device under dark/illuminated (665 nm wavelength) conditions, (b) wavelength-dependent responsivity curve of the fabricated device for visible range from 400 to 900 nm.

Figure 2.5(b) gives the maximum responsivity (R) value of 52.5 A/W at ~665 nm under -3 volt bias voltage. The minimum responsivity of 0.21972 A/W is measured at the start of the visible range of 400 nm. The dominant responsivity is observed in the range of 600-700 nm. It may be mentioned that 380-780 nm wavelengths are considered for VLC applications [120][115]. The responsivity characteristics thus show that our proposed photodetector is suitable for color light detection in VLC systems.

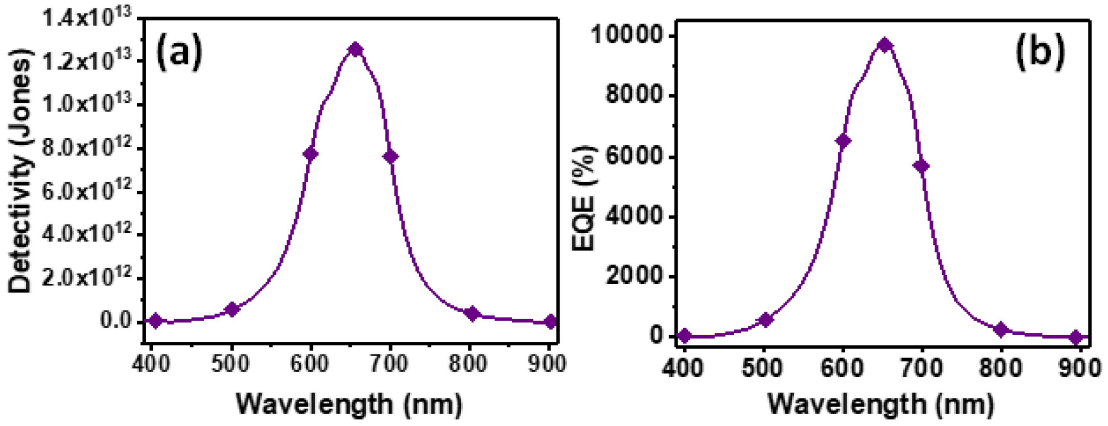

Figure 2.6 (a) Specific detectivity curve of the fabricated device for visible light spectrum, and (b) EQE curve of the fabricated device with wavelength ranging from 400 nm to 900 nm.

The EQE, a crucial parameter for any photodetectors, is defined as the ratio of the total electron-hole pairs collected at the external circuit to the number of photons incident on the device. It is mathematically expressed as [113][38]:

$$EQE\ (\%)\ = 100 \times \left[\frac{1240}{\lambda(nm)}\right] R \tag{2.3}$$

where, λ is the wavelength of the incident light.

The EQE (%) as a function of wavelength is shown in **Figure 2.6(b)**. The maximum EQE is obtained as 9789% at 665 nm and -3 V bias voltage. The high EQE above 100% is attributed to the photoconductive gain in the MSM structure[121]. The structural defects and disorders, or shallow traps in PTB7 may contribute to the photoconductive gain through band tail states in the valence and conduction bands [122].

The specific detectivity (D^*) of any photodetector represents the minimum optical signal power which the photodetector can detect successfully. Mathematically, it is calculated from the following formula [39]:

$$D^* = R \times \sqrt{\frac{A}{2\, e^-\, I_{dark}}} \tag{2.4}$$

where, I_{dark} is dark current, e^- is the charge of an electron and A is the effective area of the fabricated device.

In **Figure 2.6(a)**, the proposed photodetector's detectivity as a function of incident wavelength is shown. The maximum detectivity of ~1.28×10^{13} Jones is obtained at the incident light intensity of ~1.039 μW/cm^2 at 665 nm wavelength.

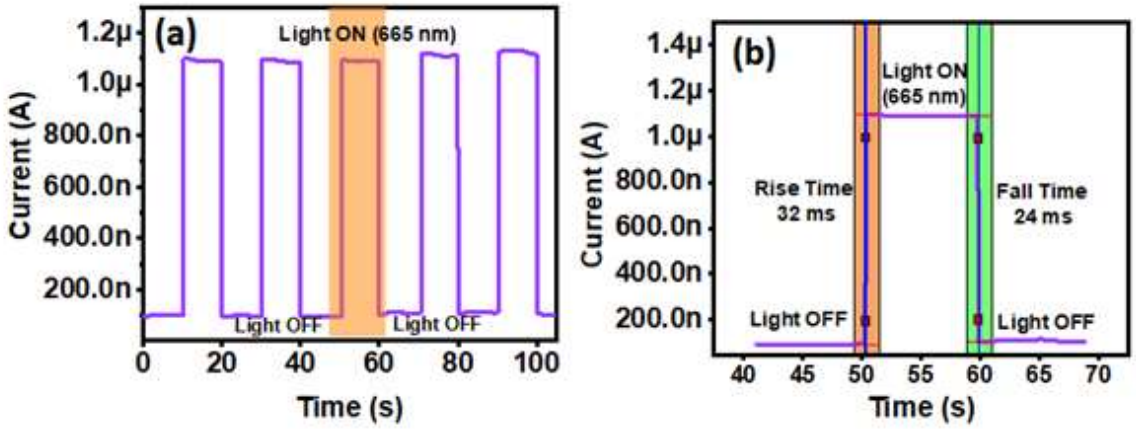

Figure 2.7 (a) Transient analysis of the fabricated device and (b) rise time and fall time calculation from single peak of wavelength 665 nm.

We will now study the transient response of the fabricated device using a light pulse (~1.039 μW/cm^2 intensity of 665 nm) of 10 sec ON/OFF periods. **Figure 2.7(a)** shows the output current of the photodetector as a function of time and **Figure 2.7(b)** shows the response for only one period of the incident ON/OFF light pulse.

The response/recovery time of the as-fabricated PTB7 polymer-based MSM photodetector is defined in terms of the rise time (i.e. time taken for changing the output current from 10% to 90% of its peak value after the light source is turned ON) and fall-time (i.e. time taken for changing the output current from 90% to 10% of its peak value after the light source is turned OFF) of the current. The minute analysis of **Figure 2.7(b)**

gives the rise-time and fall-time under -3 V bias voltage as 32 ms and 24 ms, respectively, which are believed to very good for polymer-based photodetectors. Different performance parameters of the proposed photodetector are summarized in **Table 2.1**. In **Table 2.2**, we have compared the performance parameters of our proposed PTB7-based MSM photodetector with those of other MSM photodetectors of different materials working in the visible regions. It is observed from **Table 2.2** that our device shows better performance parameter values of the responsivity, detectivity and EQE as compared to other MSM photodetectors at a reasonably very low incident illumination level.

Table 2.1 Optical parameters of fabricated photodetector

Bias (V)	Incident Light (nm)	Responsivity (A/W)	EQE (%)	Detectivity (Jones)	Rise/Fall Time (ms)
-3 V	Visible (~665 nm)	~ 52.5	9789%	~ 1.28×10^{13}	32 and 24

2.4 Working of the Device

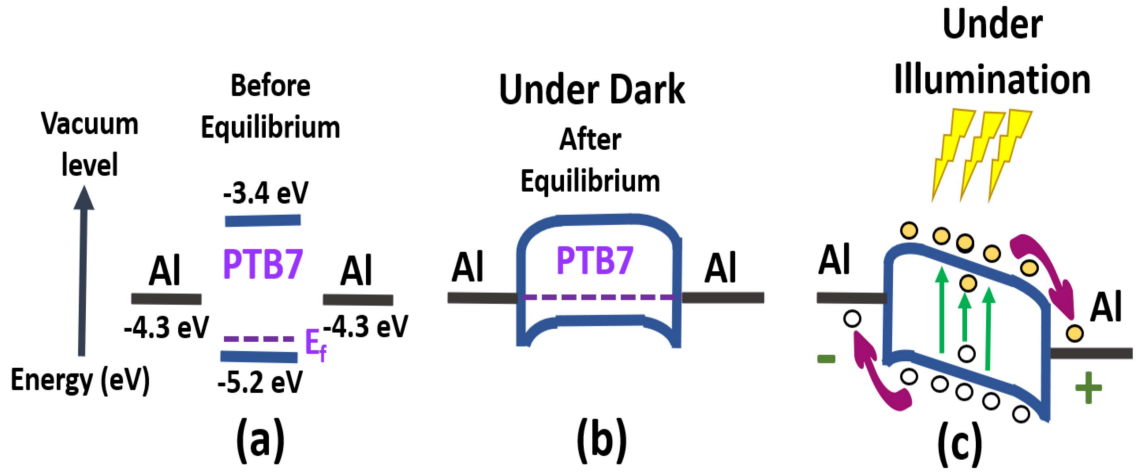

Figure 2.8 Energy band representation of the fabricated device structure (a) before equilibrium (b) at equilibrium under dark conditions and (c) under light illumination.

The energy band diagram of the Al/PTB7/Al photodetector is discussed in **Figure 2.8**. **Figure 2.8(a)** shows the energy levels of the HOMO (- 5.2 eV) and LUMO (-3.4 eV) of the PTB7 material [123] and work function energy (-4.3 eV) of the Al before the formation. The greater work function energy of PTB7 (p-type material) than the work function energy of metal indicates Schottky junctions forming MSM structure of the device. **Figure 2.8(b)** shows energy diagram of the device under dark and unbiased conditions. It is well-known that the thermionic emission is the dominant carrier transport mechanism for the dark current in the schottky photodetector. For the schottky junction between Al (with work function of -4.3 eV) and PTB7 (with energy level of LUMO of -3.4 eV) considered in the present device, it is expected to have a low dark current in our proposed device due to a reasonably high barrier height of 0.9 eV at the Al/PTB7 interface. **Figure 2.8(c)** shows the energy band diagram of the device under illumination and biased conditions. Under illumination, excess electron-hole pairs are generated in the PTB7 film due to transition of electrons from the HOMO (equivalent to the valence band in inorganic semiconductor) to the LUMO (equivalent to the conduction band of the inorganic semiconductor) due to absorption of incident photons on the device shown in **Figure 2.8(c)**. When a bias voltage is applied between two Al electrodes, the energy of the negatively electrode is increased with respect to the positively biased contact electrode as shown in the figure. As a result, electrons can easily move toward the positively biased electrode while the holes move toward the negative biased electrode as shown in **Figure 2.8(c)**. The collected electrons and holes by the respective positive and negative electrodes constitute the photocurrent in the proposed Al/PTB7/Al MSM photodetector. The structural defects and disorders, or shallow traps in PTB7 may also help in enhancing the photocurrent of our proposed PTB7 based MSM

photodetector[122]. The proposed photodetector thus gives high responsivity (R) and EQE as already discussed above.

Table 2.2 Comparison with other visible photodetector

Device Structure	Device Structure	Applied Bias (V)	Wavelength (nm)	Optical Power intensity ($\mu W/cm^2$)	Responsivity (A/W)	EQE	Detectivity (D*) (in Jones)	Rise time and fall time (in ms)
ZnO NP/$CH_3NH_3PbI_3$/PTB7 [124]	Inverted	-2	350 – 850	100×10^3	~0.36	83.6 %	~7.8×10^{12}	81 and 75
MoS_2 film [119]	MSM	-3	775	20	8.26	--	~6.5×10^{14}	1100 and 1050
Porous Si/CuO film [125]	MSM	5	532	10×10^3	0.036	--	--	800 and 800
CuO thin film [126]	MSM	5	630	5×10^3	0.059	11.6 %	2.03×10^8	5385 and 5228
$Cu_{2-x}O$ film [127]	MSM	-3	530	128	0.631	147.8 %	13.91×10^{11}	100 and 90
MoS_2 layer [128]	MSM	-10	532	2×10^6	0.57	--	~10^{10}	0.07 and 0.110
WS_2 film [129]	MSM	2	512	580	1.76	565.2 %	8.97×10^{11}	~100 and 100
InAlN film [130]	MSM	5	520	--	0.67	--	--	620 and 630
TlInSSe film [131]	MSM	10	532	300	0.61	120%	6.24×10^{11}	310 and 300
V_2O_5 nanorods[117]	MSM	5	540	1.5×10^3	0.94	--	--	787 and 541
Al/PTB7/SiO_2/Si [**Proposed work**]	MSM	-3	~665	~1.039	52.5	9789 %	1.28×10^{13}	32 and 24

2.5 Conclusion

This chapter demonstrates the fabrication and characterization of a low-cost solution-processed PTB7 polymer thin film-based Al/PTB7/Al MSM photodetector for visible light detection. The maximum responsivity, EQE and detectivity are measured as 52.5 A/W, 9789%, ~1.28×10^{13} Jones, respectively, at ~665 nm wavelength under -3 V bias. The rise time is measured as 32 ms and fall time is obtained as 24 ms. The proposed structure can be used for VLC applications.